OPEN ACCESS
Fractals, Vol. 28, No. 8 (2020) 2040010 (12 pages)
© The Author(s)
DOI: 10.1142/S0218348X20400101

World Scientific
www.worldscientific.com

Fractals 2020.28. Downloaded from www.worldscientific.com
by 157.51.20.200 on 08/09/21. Re-use and distribution is strictly not permitted, except for Open Access articles.

THE REPRODUCING KERNEL ALGORITHM FOR NUMERICAL SOLUTION OF VAN DER POL DAMPING MODEL IN VIEW OF THE ATANGANA–BALEANU FRACTIONAL APPROACH

SHAHER MOMANI,[*,†,§] BANAN MAAYAH[†,¶] and OMAR ABU ARQUB[‡,‖]
[*]*Department of Mathematics and Sciences*
College of Humanities and Sciences
Ajman University, Ajman, UAE
[†]*Department of Mathematics, Faculty of Science*
The University of Jordan, Amman 11942, Jordan
[‡]*Department of Mathematics, Faculty of Science*
Al-Balqa Applied University, Salt 19117, Jordan
[§]*s.momani@ajman.ac.ae; s.momani@ju.edu.jo*
[¶]*b.maayah@ju.edu.jo*
[‖]*o.abuarqub@bau.edu.jo*

Received January 7, 2020
Accepted March 3, 2020
Published September 1, 2020

Abstract

The aim of this paper is to propose the Atangana–Baleanu fractional methodology for fathoming the Van der Pol damping model by using the reproducing kernel algorithm. To this end, we discuss the mathematical structure of this new approach and some other numerical properties of solutions. Furthermore, all needed requirements for characterizing solutions by applying the reproducing kernel algorithm are debated. In this orientation, modern trend and new computational algorithm in terms of analytic and approximate Atangana–Baleanu fractional solutions

‖Corresponding author.
This is an Open Access article in the "Special Issue on Fractal and Fractional with Applications to Nature" published by World Scientific Publishing Company. It is distributed under the terms of the Creative Commons Attribution 4.0 (CC BY) License which permits use, distribution and reproduction in any medium, provided the original work is properly cited.

are proposed. Finally, numerical simulations in fractional emotion is constructed one next to the other with tabulated data and graphical portrayals.

Keywords: Atangana–Baleanu Fractional Derivative; Van der Pol Damping Model; Reproducing Kernel Algorithm.

Fractals 2020.28. Downloaded from www.worldscientific.com
by 157.51.20.200 on 08/09/21. Re-use and distribution is strictly not permitted, except for Open Access articles.

1. INTRODUCTION

Fractional calculus theory is a part of mathematical analysis, widely explored in the ongoing years, has risen as a viable and amazing asset for the scientific demonstrating of engineering and scientific phenomena.[1–5] In realm of derivatives; the analytics approaches of fractional calculus theory are significantly based on Riemann–Liuoville or Caputo–Liuoville versions, these versions are mostly addressed in scientific researches in the last few years.[6–13] The most common likeness among these two versions are abstracted in singularity and nonlocal kernel functions manifest in the integral operators.[1–13] But no one denies that, the most natural and fruitful definition should be come from the real-world marvels that modeled from fractional dynamic issues. To deal with these reversals, a new construction for fractional derivative, so called, Atangana–Baleanu–Caputo (ABC) is presented hither.[14] This fractional ABC derivative seems to be liberate of singularity with local kernel function, because the kernel depends on the exponential function. Aught, this definition is elaborated upon with its special properties strongly and heavily in the recent times as utilized in Refs. 15–26.

To customize more, beneath of the ABC differentiability agency, we will discuss the ABC fractional Van der Pol (VDP) damping model. Meanwhile, reproducing kernel algorithm (RKA) of Hilbert space within some characterization theorems are also utilized. To select more, those analyses employed the discussions about the VDP model of the accompanying form:

$$\begin{cases} \dfrac{{}^{ABC}_{t_0}d^{\beta}u(t)}{dt^{\beta}} + \mu(u^2(t)-1)\dfrac{du(t)}{dt} + u(t) = h(t), \\ u\left(t_0\right) = \mathcal{P}, \\ \dfrac{du\left(t_0\right)}{dt} = \mathcal{P}'. \end{cases} \tag{1}$$

Extremely, we will symbolize the following: $t_0 \in [t_0, T]$; $\beta \in (1, 2]$; $\mu > 0$; $T, \mathcal{P}, \mathcal{P}' \in \mathbb{R}$; $\mathbb{A} := [t_0, T]$; and $u, h \in C(\mathbb{A}, \mathbb{R})$. Hither, $\frac{{}^{ABC}d^{\beta}u(t)}{dt^{\beta}}$ denotes to ABC fractional derivative of u in t over $\mathbb{A}$ of order β and is given as

$$\frac{{}^{ABC}_{t_0}d^{\beta}u(t)}{dt^{\beta}} = \frac{1-\beta+\beta\Gamma^{-1}(\beta)}{1-\beta}\int_{t_0}^{t}\frac{d^2u\left(\tau\right)}{dt^2} \times L_{\beta}\left(-\frac{\beta}{1-\beta}\left(t-\tau\right)^{\beta}\right)d\tau, \tag{2}$$

in which t_0 is a base point acquaint at $t \in \mathbb{A} - \{t_0, T\}$ and $u \in \mathrm{Z}^2(\mathbb{A} - \{t_0, T\})$. Whereas, $L_{\beta}(t) = \sum_{n=0}^{\infty}\frac{1}{\Gamma(n\beta+1)}t^n$ with $\beta > 0$ and $t \in \mathbb{R}$ is the Mittag-Leffler function and $\mathrm{Z}^2\left(\mathbb{A} - \{t_0, T\}\right)$ is the Sobolev space of order 2 on the domain $\mathbb{A} - \{t_0, T\}$ and is defined as

$$\mathrm{Z}^2(\mathbb{A} - \{t_0, T\}) = \left\{ z \in L^2(\mathbb{A} - \{t_0, T\}) : \frac{dz(t)}{dt}, \frac{\mathrm{d}^2 z(t)}{dt^2} \in L^2(\mathbb{A} - \{t_0, T\}) \right\}. \tag{3}$$

The VDP evolution model in Eq. (1) with time $t \in A$ is a fractional second-order nonlinear damping equation which introduced in Ref. 27 and elaborated upon with its special properties in Refs. 28–33 to describe the oscillation of triode in the electrical circuit. Here, $u(t)$ is the position coordinate elucidated as function of time and μ is the control parameter which indicates the nonlinearity and the strength of the damping. Note that, when $\mu = 0$, then there is no damipng force and the VDP model conserves energy. When $0 < \mu < 1$, then the auto oscillations of the VDP oscillator are close to simple harmonic oscillations. Whilst , with increasing μ; the auto oscillations deviate more and more from harmonic oscillations and the VDP model will enter a limit cycle.

This analysis is stamped by expanding the RKA implementation areas as a novel numerical solver for the VDP damipng model. The RKA main area topic is in mathematical modeling and numerical simulation of multidimensional issues arising in engineering and physical sciences.[34–36] As a rule, such

Fractals 2020.28. Downloaded from www.worldscientific.com by 157.51.20.200 on 08/09/21. Re-use and distribution is strictly not permitted, except for Open Access articles.

issues are governed by linear and nonlinear integral-differential operators that requires novel mathematical analysis together with numerical algorithms. The RKA particular interest is in the design of new mathematical analysis and numerical algorithm for solving such operator equations involving strong nonlinearity and discontinuity shapes.[37–42]

In addition to the introduction, the residual synopsis of the paper is structured in the following subsidiary sections, simultaneously. The mathematical structures of RKA: requirements use, principles, and tools. Exemplification of the VDP Solution: formulation and algorithm. Convergence and Error Structures: solution behavior and characterization theorems. Numerical applications and computational results: RKA steps, test applications, and extensive discussions. Finally, succinct highlight and conclusion are given on record.

2. MATHEMATICAL STRUCTURES OF THE RKA

The hypothesis of reproducing kernel has been considered and exhibited broadly; despite the fact that the RKA instruments have for some time been known and applied in different utilizations of engineering and science.[34–58] At all events the RKA is an effective approach for solving wide class of differential-integral operator equations in the fractional emotion and provided a general numeric scheme to handle the solution behaviors. Extremely, we will symbolize $|C|(\mathbb{A})$ to denote the set of absolutely continuous functions on $\mathbb{A}$.

Let $\mathcal{H}$ be a Hilbert space of functions defined on $\mathbb{A}$. A function $\Psi \in \mathrm{C}(\mathbb{A}\times\mathbb{A},\mathbb{R})$ is a reproducing kernel of K if it fulfills the subsequent requirments:

- $\forall t \in \Lambda : \Psi(\bullet, t) \in \mathcal{H}$;
- $\forall \psi \in \mathcal{H}$ and $\forall t \in \mathbb{A}$: $\langle \psi(\cdot), \Psi(\cdot, t)\rangle_{\mathcal{H}} = \psi(t)$.

Definition 1 (see Ref. 18). The Hilbert space $\mathcal{W}(\mathbb{A})$ is arranged as

$$\mathcal{W}(\mathbb{A}) = \left\{ u(t) : u(t), \frac{du(t)}{dt}, \frac{d^2u(t)}{dt^2} \in |C|(\mathbb{A}); \frac{d^3u(t)}{dt^3} \in L^2(\mathbb{A}); u(t_0) = \frac{du(t_0)}{dt} = 0 \right\} \quad (4)$$

against the additional functional structure

$$\langle u(t), v(t)\rangle_W = \sum_{i=0}^{2} \frac{d^i u(t_0)}{dt^i}\frac{d^i v(t_0)}{dt^i} + \int_{\mathbb{A}} \frac{d^3u(t)}{dt^3}\frac{d^3v(t)}{dt^3}dt, \quad (5)$$

$$\|u(t)\|_{\mathcal{W}} = \sqrt{\langle u(t), u(t)\rangle_{\mathcal{W}}}. \quad (6)$$

Definition 2 (see Ref. 18). The Hilbert space $\mathcal{V}(\mathbb{A})$ is arranged as

$$\mathcal{V}(\mathbb{A}) = \left\{ u(t) : u(t) \in |C|(\mathbb{A}); \frac{du(t)}{dt} \in L^2(\mathbb{A}) \right\}, \quad (7)$$

against the additional functional structure

$$\langle u(t), v(t)\rangle_{\mathcal{V}} = \int_{\mathbb{A}} \left(u(t)v(t) + \frac{du(t)}{dt}\frac{dv(t)}{dt} \right) dt, \quad (8)$$

$$\|u(t)\|_{\mathcal{V}} = \sqrt{\langle u(t), u(t)\rangle_{\mathcal{V}}}. \quad (9)$$

Theorem 1 (see Ref. 18). *The Hilbert space $W(\mathbb{A})$ is a complete reproducing kernel with kernel function $\mathcal{G}_t(s)$, where*

$$\mathcal{G}_t(s) = \begin{cases} \mathcal{G}(t,s), & s \le t, \\ \mathcal{G}(s,t), & s > t, \end{cases} \quad (10)$$

so that $\mathcal{G}(t,s) = \frac{1}{120}(t_0 - s)^2(-6t_0^3 - 5s^2t + \mathrm{s}^3 + 10t^2(3+s) + 3t_0^2(10 + s + 5t) - 2t_0(5t^2 - s^2 + 5t(6 + s)))$.

Theorem 2 (see Ref. 18). *The Hilbert space $\mathcal{V}(\mathbb{A})$ is a complete reproducing kernel with kernel function $\mathcal{H}_t(s)$, where*

$$\mathcal{H}_t(s) = \begin{cases} \mathcal{H}(t,s), & s \le t, \\ \mathcal{H}(s,t), & s > t, \end{cases} \quad (11)$$

so that $\mathcal{H}(t,s) = \frac{1}{2}\mathrm{csch}(T - t_0)(\cosh(t + s - T - t_0) + \cosh(t - s - T + t_0))$.

In applicability of the RKA, we divide the compact set $\mathbb{A}$ into uniform splits encoded by t_i. This assumed that the gained set $\{t_i\}_{i=1}^{\infty}$ will be dense in $\mathbb{A}$; this is due to the compactness is next best thing to being finite. Also, it remarks that compactness somehow point out that the sets are somehow not big. Anyhow, we attempt to cover the set as well as the numerical process should end up in finite phases.

Theorem 3. *The system $\{\mathcal{G}_{t_i}(s)\}_{i=1}^{\infty}$ is linearly independent in $\mathcal{W}(\mathbb{A})$.*

Fractals 2020.28. Downloaded from www.worldscientific.com
by 157.51.20.200 on 08/09/21. Re-use and distribution is strictly not permitted, except for Open Access articles.

Proof. The validation is achieved by showing $\{\mathcal{G}_{t_i}(s)\}_{i=1}^{m}$ is linearly independent $\forall m \geq 1$. If $\{\sigma_i\}_{i=1}^{m}$ is picked so that $\sum_{i=1}^{m}\sigma_i\mathcal{G}_{t_i}(s) = 0$, taking $h_k(s) \in \mathcal{W}(\mathbb{A})$ such that $h_k(s_l) = \delta_{l,k}$ for each $l = 1, 2, \ldots, m$, then for each $k = 1, 2, \ldots, m$

$$\begin{aligned} 0 &= \left\langle h_k(s), \sum_{i=1}^{m}\sigma_i\mathcal{G}_{t_i}(s)\right\rangle_W \\ &= \sum_{i=1}^{m}\sigma_i\langle h_k(s), \mathcal{G}_{t_i}(s)\rangle_W \\ &= \sum_{i=1}^{m}\sigma_i h_k(s_i) = \sigma_i. \end{aligned} \tag{12}$$

□

The main tools in the RKA are the subsequent requirements: building appropriate Hilbert spaces, generating corresponding kernel functions, defining appropriate differential linear operator, fitting orthonormal function systems, collecting symbolic computations and datasets, and software mathematical package solver. In the next subsection, the RKA is developing to construct highly efficient numerical solutions for the VDP damping model that arise in the engineering and physical sciences and combine the implementations in a user-friendly framework.

3. EXEMPLIFICATION OF THE VDP MODEL SOLUTION

In this cutter, we derive the robust formulation of the problem with a view to solve it using the RKA. Some demanded theoretical results regarding the orthogonal function system, completeness, and exemplification of the ABC analytic and approximate solutions are supplied in $\mathcal{W}(\mathbb{A})$ and $\mathcal{V}(\mathbb{A})$.

Hither in our formalism, we will consider the VDP damping model exclusively. Be that as it may, before continuing further, we need the accompanying transformation so as to fix the necessary solutions in the domain space $\mathcal{W}(\mathbb{A})$. For the clarity, it is convenient to apply the replacement $u(t) :\to u(t) - (\mathcal{P}'t + \mathcal{P})$ on Eq. (1). At last, we still signify the conversion solution by $u(t)$ as

$$\begin{cases} \dfrac{{}^{ABC}_{t_0}d^{\beta}u(t)}{dt^{\beta}} - \mu\dfrac{du(t)}{dt} + u(t) + \mu u^2(t)\dfrac{du(t)}{dt} \\ \quad = \bar{h}(t), \\ u(t_0) = 0, \\ \dfrac{du(t_0)}{dt} = 0. \end{cases} \tag{13}$$

Essentially, define the linear operator $\mathbb{O}$ and its map $\mathbb{O}[u](t)$ as

$$\begin{cases} \mathbb{O} : \mathcal{W}(\mathbb{A}) \to \mathcal{V}(\mathbb{A}), \\ \mathbb{O}[u](t) = \dfrac{{}^{ABC}_{t_0}d^{\beta}u(t)}{dt^{\beta}} - \mu\dfrac{du(t)}{dt} + u(t). \end{cases} \tag{14}$$

Based on this, if $\overline{\bar{h}}(t, u(t), \frac{du(t)}{dt}) := \bar{h}(t) - \mu u^2(t)\frac{du(t)}{dt}$, then Eq. (13) can be converted into the equivalent form as

$$\begin{cases} \mathbb{O}[u](t) = \overline{\bar{h}}\left(t, u(t), \frac{du(t)}{dt}\right), \\ u(t_0) = 0, \\ \dfrac{du\,(t_0)}{dt} = 0. \end{cases} \tag{17}$$

Following, we will organize and construct system of orthogonal functions using the subsequent steps: put $\mathfrak{S}_i(t) = \mathcal{H}_{t_i}(t)$ and $\mathcal{U}_i(t) = \mathbb{O}^*[\mathfrak{S}_i](t)$, $i = 1, 2, 3, \ldots$, where $\mathbb{O}^*$ is the adjoint operator of $\mathbb{O}$, and $\{t_i\}_{i=1}^{\infty}$ is dense on $\mathbb{A}$.

In Algorithm 1, the subsequent inputs are needed so as to deduce the system of orthonormal functions

Algorithm 1. To apply the Gram–Schmidt process the subsequent steps should be talking into account:

Step 1: For $i = 2, 3, \ldots,$ and $k = 1, 2, \ldots i-1$,

do the following:

$$\omega_{ik} = \begin{cases} \dfrac{1}{\|\mathcal{U}_1\|_{\mathcal{W}}}, \quad i = k = 1, \\ \dfrac{1}{\sqrt{\|\mathcal{U}_i\|_{\mathcal{W}}^2 - \sum_{p=1}^{i-1}\langle\mathcal{U}_i(t)\bar{\mathcal{U}}_p(t)\rangle_{\mathcal{W}}^2}}, \\ \qquad\qquad i = k \neq 1, \\ -\dfrac{1}{\sqrt{\|\mathcal{U}_i\|_{\mathcal{W}}^2 - \sum_{p=1}^{i-1}\langle\mathcal{U}_i(t), \bar{\mathcal{U}}_p(t)\rangle_{\mathcal{W}}^2}} \\ \quad \sum_{p=k}^{i-1}\langle\mathcal{U}_i(t), \bar{\mathcal{U}}_p(t)\rangle_{\mathcal{W}}\omega_{pk}, \quad i > k. \end{cases} \tag{15}$$

Output: The orthogonalization coefficients ω_{ik}.

Step 2: For $i = 1, 2, 3, \ldots$ set

$$\bar{\mathcal{U}}_i(t) = \sum_{k=1}^{i}\omega_{ik}\mathcal{U}_k(t). \tag{16}$$

Output: systems of orthonormal functions

$\{\bar{\mathcal{U}}_i(t)\}_{i=1}^{\infty}$.

Fractals 2020.28. Downloaded from www.worldscientific.com by 157.51.20.200 on 08/09/21. Re-use and distribution is strictly not permitted, except for Open Access articles.

$\{\bar{\mathcal{U}}_i(t)\}_{i=1}^{\infty}$: the space $\mathcal{W}(\mathbb{A})$; the counter indexes of k and i; and the form of $\mathcal{U}_i(t)$ and $\bar{\mathcal{U}}_i(t)$.

Theorem 4. *The system* $\{\mathcal{U}_i(t)\}_{i=1}^{\infty}$ *is complete and* $\mathcal{U}_i(t) = \mathbb{O}_s[\mathcal{G}_t](s)|_{s=t_i}$.

Proof. Still, if $\langle u(t), \mathcal{U}_{ij}(t)\rangle_W = 0$, $i = 1, 2, \ldots, j = 1, 2$, then

$$\begin{aligned}\langle u(t), \mathcal{U}_i(t)\rangle_W &= \langle u(t), \mathbb{O}^*[\mathfrak{S}_i](t)\rangle_{\mathcal{W}} \\ &= \langle \mathbb{O}[u](t), \mathfrak{S}_i(t)\rangle_{\mathcal{V}} \\ &= \mathbb{O}[u](t_i) \\ &= 0. \end{aligned} \tag{18}$$

Hither, $u(t) = \langle u(\cdot), \mathcal{G}_t(\cdot)\rangle_W$. Hence, $\mathbb{O}[u](t) = \langle \mathbb{O}[u](t), \mathfrak{S}_i(t)\rangle_W = 0$. By the density of $\{t_i\}_{i=1}^{\infty}$ on $\mathbb{A}$, we have got $\mathbb{O}[u](t) = 0$. During the existence of $\mathbb{O}^{-1}$, yields that $u(t) = 0$. Subsequently, $\{U_i(t)\}_{i=1}^{\infty}$ is a complete on $W(\mathbb{A})$. In the second part, visibly,

$$\begin{aligned} U_i(t) &= \mathbb{O}^*\left[\mathfrak{S}_i\right](t) \\ &= \langle \mathbb{O}^*[\mathfrak{S}_i](s), \mathcal{G}_t(s)\rangle_W \\ &= \langle \mathfrak{S}_i(s), O_s[\mathcal{G}_t](s)\rangle_H = \mathbb{O}_s[\mathcal{G}_t](s)|_{s=t_i}. \end{aligned} \tag{19}$$

□

Calling up that $\overline{\overline{h}}\left(t, u(t), \frac{du(t)}{dt}\right) := \bar{h}(t) - \mu u^2(t)\frac{du(t)}{dt}$ and we will employ this in the subsequent analysis.

Theorem 5. *Assume* ω_{ik} *are orthogonalization coefficients for the systems of orthonormal functions* $\{\bar{U}_i(t)\}_{i=1}^{\infty}$. *Then whenever* $n \to \infty$ *the analytic solution of Eq.* (17) *fulfill well*

$$u(t) = \sum_{i=1}^{\infty}\sum_{k=1}^{i}\omega_{ik}\overline{\overline{h}}\left(t_k, u(t_k), \frac{du(t_k)}{dt}\right)\bar{U}_i(t). \tag{20}$$

Proof. Because $\langle u(t), \mathfrak{S}_i(t)\rangle_W = u(t_i)$ and $\sum_{i=1}^{\infty}\langle u(t), \bar{U}_i(t)\rangle_W \bar{U}_i(t)$ is the Fourier series amplification around $\{\bar{U}_i(t)\}_{i=1}^{\infty}$. Then it is convergent in the emotion of $\|\cdot\|_W$. From here,

$$\begin{aligned} u(t) &= \sum_{i=1}^{\infty}\left\langle u(t), \bar{U}_i(t)\right\rangle_W \bar{U}_i(t) \\ &= \sum_{i=1}^{\infty}\left\langle u(t), \sum_{k=1}^{i}\omega_{ik}U_k(t)\right\rangle_W \bar{U}_i(t) \\ &= \sum_{i=1}^{\infty}\sum_{k=1}^{i}\omega_{ik}\left\langle u(t), \mathbb{O}^*\left[\mathfrak{S}_k\right](t)\right\rangle_W \bar{U}_i(t) \\ &= \sum_{i=1}^{\infty}\sum_{k=1}^{i}\omega_{ik}\langle \mathbb{O}[u](t), \mathfrak{S}_k(t)\rangle_H \bar{U}_i(t) \\ &= \sum_{i=1}^{\infty}\sum_{k=1}^{i}\omega_{ik}\left\langle \overline{\overline{h}}\left(t, u(t), \frac{du(t)}{dt}\right), \mathfrak{S}_k(t)\right\rangle_H \\ &\quad \times \bar{U}_i(t) \\ &= \sum_{i=1}^{\infty}\sum_{k=1}^{i}\omega_{ik}\overline{\overline{h}}\left(t_k, u\left(t_k\right), \frac{du\left(t_k\right)}{dt}\right)\bar{U}_i(t). \end{aligned} \tag{21}$$

Thus, $u(t)$ in Eq. (20) is the analytic solution of Eq. (17). □

For numerical computations, we truncated the series in Eq. (20) and creating the n-term numerical solution of $u(t)$ using

$$u^n(t) = \sum_{i=1}^{n}\sum_{k=1}^{i}\omega_{ik}\overline{\overline{h}}\left(t_k, u(t_k), \frac{du(t_k)}{dt}\right)\bar{U}_i(t). \tag{22}$$

The complete algorithm of finding the solution of the VDP damping model using the RKA will be given later in details in Algorithm 2 of Sec. 5.

4. CONVERGENCE AND ERROR STRUCTURES

To encompass the conduct of the numerical solutions; convergence analysyis and error conduct in the RKA are drawn. Hither, $\|u^{n-1}\|_W$ is bounded whenever $n \to \infty$ and $\{t_i\}_{i=1}^{\infty}$ is dense on $\mathbb{A}$. In the ensuing picked up results, we expected that the solution of Eq. (17) satisfies the compatibility conditions which are existence, uniqueness, and adequate differentiability in the Hilbert space $W(\mathbb{A})$. Extremely, we will symbolize $|\mathbb{A}| = T - t_0$ to denote the length of $\mathbb{A}$ by ususl metric function.

Lemma 1. *Whenever* $u \in W(\mathbb{A})$, *thereafter* $|u(t)| \leq (1 + \mathbb{A} + \frac{1}{2}\mathbb{A}^2 + \mathbb{A}^{\frac{5}{2}})\|u\|_W$, $|\frac{du(t)}{dt}| \leq (1 + \mathbb{A} + \mathbb{A}^{\frac{3}{2}})\|u\|_W$, *and* $|\frac{d^2u(t)}{dt^2}| \leq (1 + \mathbb{A}^{\frac{1}{2}})\|u\|_W$.

Proof. Hither in our proof, we will consider $|u(t)|$ exclusively (likewise proof can be applied for $|\frac{du(t)}{dt}|$ and $|\frac{d^2u(t)}{dt^2}|$). Perception that $\frac{d^2u(t)}{dt^2} - \frac{d^2u(t_0)}{dt^2} = \int_{t_0}^{t}\frac{d^3u(p)}{dp^3}dp$. If this is integrated from t_0 to t, the result is $\frac{du(t)}{dt}$ itself as

$$\begin{aligned}\frac{du(t)}{dt} - \frac{du(t_0)}{dt} - \frac{d^2u(t_0)}{dt^2}(t - t_0) \\ = \int_{t_0}^{\mathrm{t}}\left(\int_{t_0}^{u}\frac{d^3u(p)}{dp^3}dp\right)du. \end{aligned} \tag{23}$$

Fractals 2020.28. Downloaded from www.worldscientific.com by 157.51.20.200 on 08/09/21. Re-use and distribution is strictly not permitted, except for Open Access articles.

Integrate again from t_0 to t, yield that

$$u(t)-u(t_0)-\frac{du(t_0)}{dt}(t-t_0)-\frac{1}{2}\frac{d^2u(t_0)}{dt^2}(t-t_0)^2 = \int_{t_0}^{t}\left(\int_{t_0}^{v}\left(\int_{t_0}^{u}\frac{d^3u(p)}{dp^3}dp\right)du\right)dv. \quad (24)$$

So, by taking the ususl metric functions length yield that

$$|u(t)| \le |u(t_0)| + \left|\frac{du(t_0)}{dt}\right||t-t_0| + \frac{1}{2}\left|\frac{d^2u(t_0)}{dt^2}\right| \times |t-t_0|^2 + (T-t_0)^2\int_{\mathbb{A}}\left|\frac{d^3u(p)}{dp^3}\right|dp. \quad (25)$$

After rearranging the mathematical formulation, one find

$$|u(t)| \le |u(t_0)| + \left|\frac{du(t_0)}{dt}\right||\mathbb{A}| + \frac{1}{2}\left|\frac{d^2u(t_0)}{dt^2}\right||\mathbb{A}|^2 + |\mathbb{A}|^2\int_{\mathbb{A}}\left|\frac{d^3u(p)}{dp^3}\right|dp. \quad (26)$$

By using the Holder's inequality and Eq. (5), we can note the following:

$$\begin{aligned}\left|\frac{d^k u(t_0)}{dp^k}\right|_{k=0,1,2} &\le \left((u(t_0))^2 + \left(\frac{du(t_0)}{dt}\right)^2 + \left(\frac{d^2u(t_0)}{dt^2}\right)^2 + \int_{\mathbb{A}}\left(\frac{d^3u(t)}{dt^3}\right)^2 dt\right)^{\frac{1}{2}} \\ &= \|u\|_W, \quad (27)\\ \int_{\mathbb{A}}\left|\frac{d^3u(p)}{dp^3}\right|dp &\le \left(\int_{\mathbb{A}}\left(\frac{d^3u(p)}{dp^3}\right)^2 dp\int_{\mathbb{A}}(1)^2dp\right)^{\frac{1}{2}} \\ &\le (T-t_0)^{\frac{1}{2}}\left((u(t_0))^2 + \left(\frac{du(t_0)}{dt}\right)^2 + \left(\frac{d^2u(t_0)}{dt^2}\right)^2 + \int_{\mathbb{A}}\left(\frac{d^3u(t)}{dt^3}\right)^2 dt\right)^{\frac{1}{2}} \\ &= |\mathbb{A}|^{\frac{1}{2}}\|u\|_W. \quad (28)\end{aligned}$$

Thus, $|u(t)| \le \left(1+|A|+\frac{1}{2}|A|^2+|A|^{\frac{5}{2}}\right)\|u\|_W$. The remaining parts are obvious. □

Theorem 6. *Let* $\overline{\overline{h}}\left(t,u(t),\frac{du(t)}{dt}\right) \in C(\mathbb{A}\times\mathbb{R}\times\mathbb{R},\mathbb{R})$. *If* $\left\|u^{n-1}-u\right\|_W \to 0, t_n \to s$ *whenever* $n\to\infty$, *then as*

$$\overline{\overline{h}}\left(t,u^{n-1}(t_n),\frac{du^{n-1}(t_n)}{dt}\right) \xrightarrow{n\to\infty} \overline{\overline{h}}\left(t,u^{n-1}(s),\frac{du^{n-1}(\mathrm{s})}{dt}\right). \quad (29)$$

Proof. Firstly, we will prove that $u^{n-1}(t_n)\to u(s)$. Since, we can note that

$$\begin{aligned}\left|\frac{d^k u^{n-1}(t_n)}{dt^k}-\frac{d^k u(s)}{dt^k}\right|_{k=0,1} &= \left|\frac{d^k u^{n-1}(t_n)}{dt^k}-\frac{d^k u^{n-1}(s)}{dt^k} + \frac{d^k u^{n-1}(s)}{dt^k}-\frac{d^k u(s)}{dt^k}\right| \\ &\le \left|\frac{d^k u^{n-1}(t_n)}{dt^k}-\frac{d^k u^{n-1}(s)}{dt^k}\right| + \left|\frac{d^k u^{n-1}(s)}{dt^k}-\frac{d^k u(s)}{dt^k}\right| \\ &\le \left|\frac{d^{k+1}u^{n-1}(\xi)}{dt^{k+1}}\right||t_n-s| + \left|\frac{d^k u^{n-1}(s)}{dt^k}-\frac{d^k u(s)}{dt^k}\right| \\ &\le \left(1+\mathbb{A}+\frac{1}{2}\mathbb{A}^2+\mathbb{A}^{\frac{5}{2}}\right)\left\|u^{n-1}-u\right\|_W + \mathbb{O}(\mathbb{A})\left\|u^{n-1}\right\|_W|t_n-s|, \quad (30)\end{aligned}$$

where ξ in between $(\min\{t_n,s\},\max\{t_n,s\})$ and $\mathbb{O}(\mathbb{A}) = \{^{1+\mathbb{A}+\mathbb{A}^{\frac{3}{2}},\,k=0,}_{1+\mathbb{A}^{\frac{1}{2}},\,k=1.}$ It pursue that $|u^{n-1}(t_n)-u(s)| \to 0$ whenever $n\to\infty$. By means of $\overline{\overline{h}}(t,u(t),\frac{du(t)}{dt}) \in C(\mathbb{A}\times\mathbb{R}\times\mathbb{R},\mathbb{R})$ it implies the demanded. □

Next, we will symbolize $\mathbb{B}_i = \sum_{k=1}^{i}\omega_{ik}\times \overline{\overline{h}}(t_k,u(t_k),\frac{du(t_k)}{dt})$. In fact, this allows one to put $u^n(t)$ as

$$u^n(t) = \sum_{i=1}^{n}\mathbb{B}_i\bar{U}_{ij}(t). \quad (31)$$

Theorem 7. *In the iterative formula of Eq.* (31), *one has* $u^n(t)\to u(t)$ *whenever* $n\to\infty$.

Fractals 2020.28. Downloaded from www.worldscientific.com
by 157.51.20.200 on 08/09/21. Re-use and distribution is strictly not permitted, except for Open Access articles.

Proof. The proof gained straightway depending on $u^{n+1}(t) = u^n(t) + \mathbb{B}_{n+1}\bar{U}_{n+1}(t)$; orthogonality of $\{\bar{U}_i(t)\}_{i=1}^{\infty}$; and completeness of $W(\mathbb{A})$ that is equipped by $\|\cdot\|_W$. □

To ensure that the error will decreasing for large n, the subsequent fact is necessary. Extremely, we will symbolize $\mathbb{E}_n = \|u - u^n\|_W$ on $\mathbb{A}$ as long as $u(t)$ and $u^n(t)$ are extracted from Eqs. (21) and (22), simultaneously.

Theorem 8. *The sequence of error $\{\mathbb{E}_n\}_{n=1}^{\infty}$ is decreasing in $W(\mathbb{A})$ and $\mathbb{E}_n \to 0$ whenever $n \to \infty$.*

Proof. It apparent that

$$\begin{aligned} E_n^2 &= \left\| \sum_{i=n+1}^{\infty} \langle u(t), \bar{U}_i(t)\rangle_W \bar{U}_i(t) \right\|_W^2 \\ &= \sum_{i=n+1}^{\infty} \langle u(t), \bar{U}_i(t)\rangle_W^2 \\ &\leq \sum_{i=n}^{\infty} \langle u(t), \bar{U}_i(t)\rangle_W^2 \\ &= \left\| \sum_{i=n}^{\infty} \langle u(t), \bar{U}_i(t)\rangle_W \bar{U}_i(t) \right\|_W^2 \\ &= \mathbb{E}_{n-1}^2. \end{aligned} \tag{32}$$

Consequently, $\{\mathbb{E}_n\}_{n=1}^{\infty}$ is decreasing in $\|\cdot\|_W$. From Theorem 12, using the convergent fact on $\sum_{i=1}^{\infty} \langle u(t), \bar{U}_i(t)\rangle_W \bar{U}_i(t)$ yields that $\mathbb{E}_n^2 \to 0$ whenever $n \to \infty$. □

5. NUMERICAL APPLICATIONS AND COMPUTATIONAL RESULTS

The inferred analytical formalism is computationally decided not exclusively to verify the theoretical statements but also to match the numerical data acquired with the true solutions identified and to confirm the effectiveness of the method used. To confirm the high degree of accurateness and reliability of the proposed method, some numerical experiments within one geometries are performed.

5.1. The RKA Steps

Promoting software package is very substantial issue in the topic of numerical analysis and its real-world applications such as those arising and growing in applied mathematicd, physical, and engineering problems. The next algorithm focussing on the computational steps is required for solving VDP of Eq. (1).

Algorithm 2. Steps of RKA for numerical reckonings of VDP in case of ABC approach.

Step I: Fixed t, s in $\mathbb{A}$ and do Phases 1 and 2:
- **Phase 1:** Set $t_i = t_0 + \frac{T-t_0}{n} i$ in the indices $i = 0, 1, \ldots, n$.
- **Phase 2:** Set $U_i(t) = \mathbb{O}_s[\mathcal{G}_t](s)|_{s=t_i}$ in the indices $i = 1, 2, \ldots, n$.

Output: the orthogonal function system $U_i(t)$.

Step II: In the indices $i = 1, 2, \ldots$ and $k = 1, 2, \ldots, i-1$ do Algorithm 1.

Output: the orthogonalization coefficients ω_{ik}.

Step III: Set $\bar{U}_i(t) = \sum_{k=1}^{i} \omega_{ik} U_k(t)$ in the indices $i = 1, 2, \ldots, n$.

Output: the orthonormal function system $\bar{U}_i(t)$.

Step IV: Set $u^0(t_1) = 0$ and in the index $i = 1, 2, \ldots, n$ do Phases 1, 2, and 3:
- **Phase 1:** Set $u^i(t_i) = u^{i-1}(t_i)$.
- **Phase 2:** Set $\mathbb{B}_i = \sum_{k=1}^{i} \omega_{ik} \overline{\overline{h}}(t_k, u(t_k), \frac{du(t_k)}{dt})$.
- **Phase 3:** Set $u^n(t) = \sum_{k=1}^{i} \mathbb{B}_k \bar{U}_k(t)$.

Output: The n-term numerical reckoning $u^n(t)$ of $u(t)$.

In Algorithm 2, the subsequent inputs are needed so as to deduce the numerical reckoning u^n of u: n collocation points; independent domain A; reproducing kernel function $\mathcal{G}_t(s)$; operator $\mathbb{O}$; the space $W(\mathbb{A})$.

In all numerical results and graphical representations, the number n is taking to be 21. For this intent, Mathematics 9 programming bundle is actualized to create all the numerical reckonings and graphical outcomes.

5.2. Test Applications

To fill our presented results in the form of realistic and tangible models, three applications of damping VDP models contains forcing term in its non-homogeneous part are discussed hither. The readers should be note thither that in the next three applications, the values of $t_0 = 0$. But be sure thither this does not effect on the gained numerical results, because, the analytical solution and its derivative are known at $t_0 = 0$ which is $u(0) = \mathcal{P}$ and $\frac{du(0)}{dt} = \mathcal{P}'$ for specific one in those applications. in the subsequent three applications the VDP

models are with nonhomogeneous forcing term and $\mathbb{A} := [0, 1]$.

Application 1. Essentially, let allow us behold the subsequent VDP model:

$$\begin{cases} \frac{{}^{ABC}_{t_0}d^{\beta}u(t)}{dt^{\beta}} + (u^2(t) - 1) \\ \quad \frac{X\,du(t)}{dt} + u(t) = \sin^3(t), \\ u(0) = 1, \\ \frac{du(0)}{dt} = 0, \end{cases} \tag{33}$$

with the analytic solution when $\beta = 1$ is computed as

$$u(t) = \cos(t). \tag{34}$$

Application 2. Now, let allow us behold the subsequent VDP model:

$$\begin{cases} \frac{{}^{ABC}_{t_0}d^{\beta}u(t)}{dt^{\beta}} + 0.5(u^2(t) - 1)\frac{du(t)}{dt} + u(t) \\ \quad = \cos^3(t), \\ u(0) = 0, \\ \frac{du(0)}{dt} = -1, \end{cases} \tag{35}$$

with the analytic solution when $\beta = 1$ is computed as

$$u(t) = -\sin(\mathrm{t}). \tag{36}$$

Application 3. Finally, let allow us behold the subsequent VDP model:

$$\begin{cases} \frac{{}^{ABC}_{t_0}d^{\beta}u(t)}{dt^{\beta}} + 2\left(u^2(t) - 1\right)\frac{du(t)}{dt} + u(t) \\ \quad = -2\cos^3(t), \\ u(0) = 0, \\ \frac{du(0)}{dt} = 1, \end{cases} \tag{37}$$

with the analytic solution when $\beta = 1$ is computed as

$$u(t) = \sin(t). \tag{38}$$

In those three applications, the researchers should note that the absence of analytic solutions does not have much effect on the gained results because we will obtain and plot the numerical solutions at different values of β.

5.3. Results and Discussions

Taking $t_i = \frac{i}{n}$ in the indices $i = 0, 1, \ldots, n = 21$ on $\mathbb{A}$ in $u^n(t_i)$. Applying Algorithms 1 and 2 over the reckonings, a collection of numerical reckonings results are tabulted in the form of tables data one next to the other with some graphical portrayals. Anyhow, we apply the RKA to discudded the previous three aplications in which $t \in \mathbb{A}$, $\beta \in [1, 2] - \{1\}$. The major advantage for numerical techniques is that a numerical solution can be found even when no true solution can be gained (no solution can be obtained by hand using classical techniques).

Following, numerical validations for different values of grid points t_i when $\beta = 1$ will be exhibited. Tables 1 tabulates $u(t_i)$, $u^{21}(t_i)$, $|u(t_i) - u^{21}(t_i)|$, and $|u(t_i) - u^{21}(t_i)||u(t_i)|^{-1}$ for Application 1. Whilst Tables 2 and 3 tabulates the same outcomes for Applications 2 and 3, simultaneously. Of the results

Table 1 Numerical Results of Damping VDP Model in Applications 1 in the Case of $\beta = 1$ Using RKA.

t_i	$u(t_i)$	$u^{21}(t_i)$	$\lvert u(t_i) - u^{21}(t_i)\rvert$	$\lvert u(t_i) - u^{21}(t_i)\rvert\lvert u(t_i)\rvert^{-1}$
0	1	1.	0	0
0.1	0.9950041653	0.9950041652	$4.264422149 \times 10^{-11}$	$4.285833464 \times 10^{-11}$
0.2	0.9800665778	0.9800665764	$1.453625442 \times 10^{-9}$	$1.483190505 \times 10^{-9}$
0.3	0.9553364891	0.9553364836	$5.504406375 \times 10^{-9}$	$5.761746189 \times 10^{-9}$
0.4	0.9210609940	0.9210609802	$1.377556413 \times 10^{-8}$	$1.495619098 \times 10^{-8}$
0.5	0.8775825619	0.8775825348	$2.705135149 \times 10^{-8}$	$3.082485075 \times 10^{-8}$
0.6	0.8253356149	0.8253355690	$4.587717739 \times 10^{-8}$	$5.558608712 \times 10^{-8}$
0.7	0.7648421873	0.7648421169	$7.036426197 \times 10^{-8}$	$9.199840587 \times 10^{-8}$
0.8	0.6967067093	0.6967066091	$1.002127575 \times 10^{-7}$	$1.438377960 \times 10^{-7}$
0.9	0.6216099683	0.6216098336	$1.347095979 \times 10^{-7}$	$2.167108071 \times 10^{-7}$
1.0	0.5403023059	0.5403022605	$4.538946463 \times 10^{-8}$	$8.400753456 \times 10^{-8}$

Fractals 2020.28. Downloaded from www.worldscientific.com by 157.51.20.200 on 08/09/21. Re-use and distribution is strictly not permitted, except for Open Access articles.

Table 2 Numerical Results of Damping VDP Model in Applications 2 in the Case of $\beta = 1$ Using RKA.

t_i	$u(t_i)$	$u^{21}(t_i)$	$\lvert u(t_i) - u^{21}(t_i)\rvert$	$\lvert u(t_i) - u^{21}(t_i)\rvert \lvert u(t_i)\rvert^{-1}$
0	0	0	0	∞
0.1	−0.0998334166	−0.0998336700	$2.533063334 \times 10^{-7}$	$2.537290036 \times 10^{-6}$
0.2	−0.1986693308	−0.1986696316	$3.008487212 \times 10^{-7}$	$1.514318894 \times 10^{-6}$
0.3	−0.2955202067	−0.2955205126	$3.059637851 \times 10^{-7}$	$1.035339643 \times 10^{-6}$
0.4	−0.3894183423	−0.3894186421	$2.997580434 \times 10^{-7}$	$7.697584086 \times 10^{-7}$
0.5	−0.4794255386	−0.4794258216	$2.830006011 \times 10^{-7}$	$5.902910428 \times 10^{-7}$
0.6	−0.5646424734	−0.5646427302	$2.568052611 \times 10^{-7}$	$4.548103856 \times 10^{-7}$
0.7	−0.6442176872	−0.6442179102	$2.229895086 \times 10^{-7}$	$3.461399975 \times 10^{-7}$
0.8	−0.7173560909	−0.7173562748	$1.838699517 \times 10^{-7}$	$2.563161504 \times 10^{-7}$
0.9	−0.7833269096	−0.7833270516	$1.419963676 \times 10^{-7}$	$1.812734451 \times 10^{-7}$
1.0	−0.8414709848	−0.8414709203	$6.448104573 \times 10^{-8}$	$7.662895916 \times 10^{-8}$

Table 3 Numerical Results of Damping VDP Model in Applications 3 in the Case of $\beta = 1$ Using RKA.

t_i	$u(t_i)$	$u^{21}(t_i)$	$\lvert u(t_i) - u^{21}(t_i)\rvert$	$\lvert u(t_i) - u^{21}(t_i)\rvert \lvert u(t_i)\rvert^{-1}$
0	0	0	0	
0.1	0.0998334166	0.0998331984	$2.182690584 \times 10^{-7}$	$2.186332651 \times 10^{-6}$
0.2	0.1986693308	0.1986690852	$2.488048446 \times 10^{-7}$	$1.252356585 \times 10^{-6}$
0.3	0.2955202067	0.2955199898	$2.168816552 \times 10^{-7}$	$7.338978869 \times 10^{-7}$
0.4	0.3894183423	0.3894181468	$1.954741093 \times 10^{-7}$	$5.019643096 \times 10^{-7}$
0.5	0.4794255386	0.4794253683	$1.703496845 \times 10^{-7}$	$3.553204215 \times 10^{-7}$
0.6	0.5646424734	0.5646423299	$1.434609767 \times 10^{-7}$	$2.540740086 \times 10^{-7}$
0.7	0.6442176872	0.6442175739	$1.133670495 \times 10^{-7}$	$1.759763070 \times 10^{-7}$
0.8	0.7173560909	0.7173560110	$7.992632467 \times 10^{-8}$	$1.114179216 \times 10^{-7}$
0.9	0.7833269096	0.7833268663	$4.329563852 \times 10^{-8}$	$5.527148115 \times 10^{-8}$
1.0	0.8414709848	0.8414709805	$4.313588486 \times 10^{-9}$	$5.126247446 \times 10^{-9}$

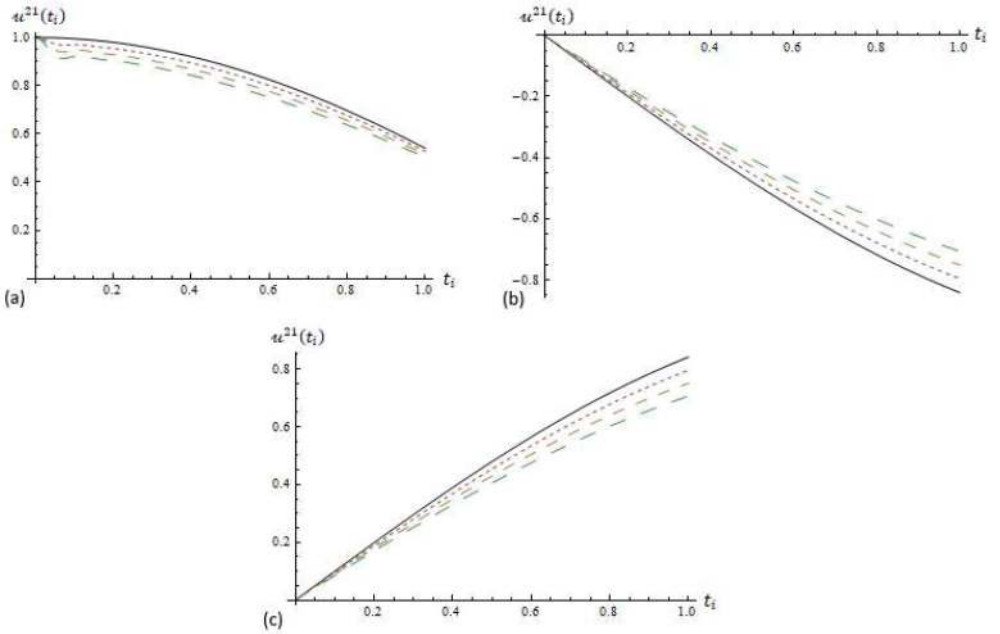

Fig. 1 Comparisons between the computational values of the RKA when $\beta \in \{0.7, 0.8, 0.9, 1\}$ and $t_i \in \mathbb{A}$: green dashed line: $\beta = 0.7$; gold dashed line: $\beta = 0.8$; dotted line: $\beta = 0.9$; solid line: $\beta = 1$ for: **(a)** Application 1; **(b)** Application 2; and **(c)** Application 3.

Fractals 2020.28. Downloaded from www.worldscientific.com
by 157.51.20.200 on 08/09/21. Re-use and distribution is strictly not permitted, except for Open Access articles.

gained, it can be observed that the full accuracy of error estimation for numerical solutions is closely related to filling t_i, so that more accurate numeric solutions can be obtained by utilizing more grid-points. Anyhow, there is good harmony and agreement between the proposed method and the numerical results.

The dynamic and geometric behaviors along the memory and heritage characteristics of the RKA are researched. Following, geometrical validations for different values of grid points $t_i \in \mathbb{A}$ and

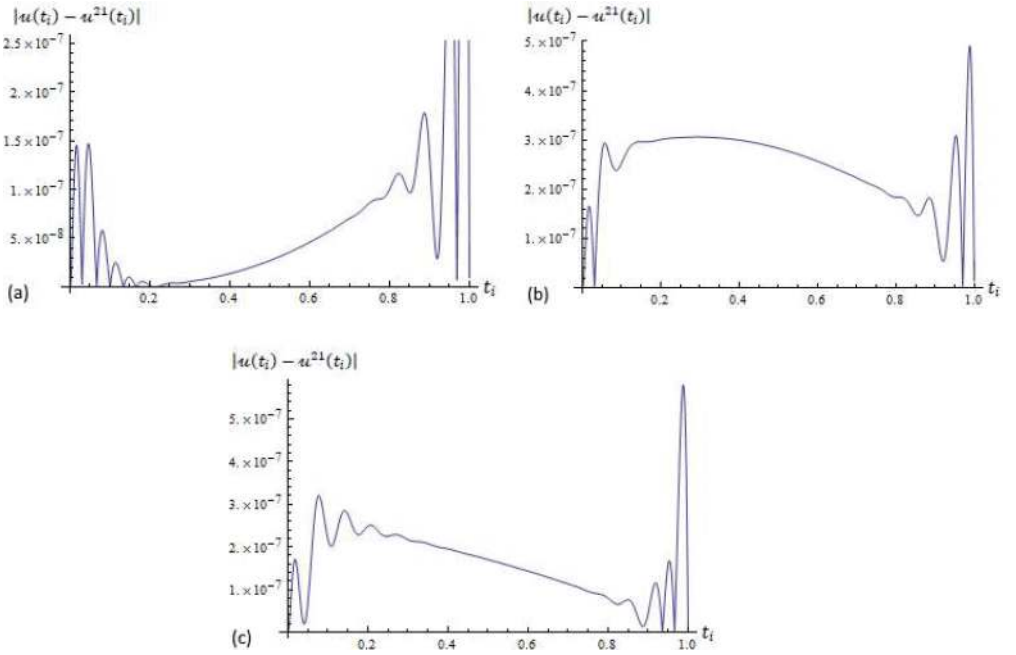

Fig. 2 Computational values of $|u(t_i) - u^{21}(t_i)|$ using the RKA when $\beta = 1$ and $t_i \in \mathbb{A}$ for: **(a)** Application 1; **(b)** Application 2; and **(c)** Application 3.

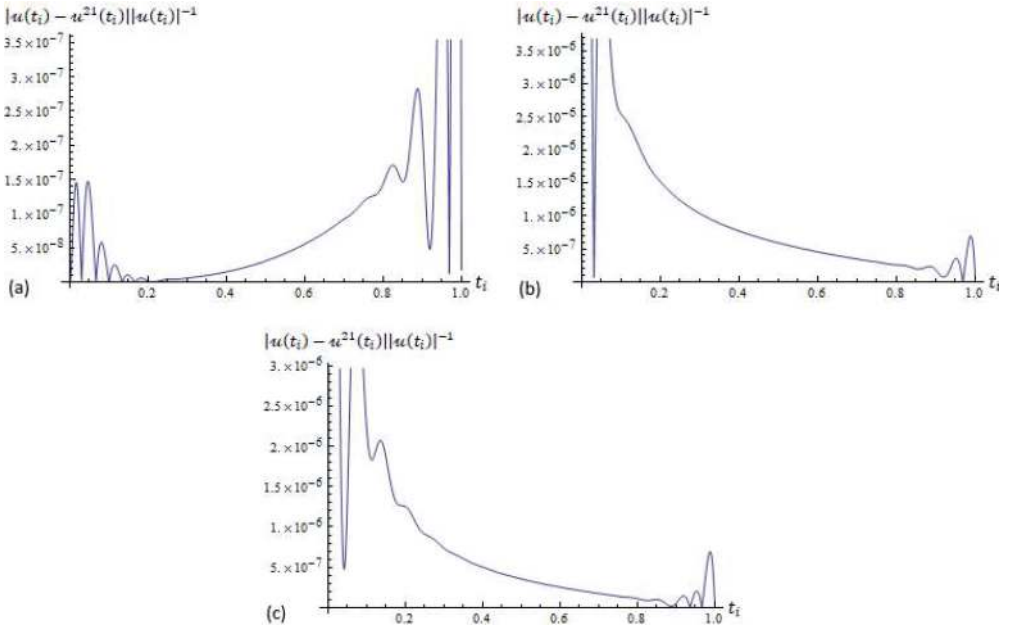

Fig. 3 Computational values of $|u(t_i) - u^{21}(t_i)||u(t_i)|^{-1}$ using the RKA when $\beta = 1$ and $t_i \in A$ for: **(a)** Application 1; **(b)** Application 2; and **(c)** Application 3.

Fractals 2020.28. Downloaded from www.worldscientific.com
by 157.51.20.200 on 08/09/21. Re-use and distribution is strictly not permitted, except for Open Access articles.

Fractals 2020.28. Downloaded from www.worldscientific.com
by 157.51.20.200 on 08/09/21. Re-use and distribution is strictly not permitted, except for Open Access articles.

$\beta \in [1,2] - \{1\}$ will be exhibited. Figure 1 tabulates the values that approximating the solutions in Applications 1, 2, and 3, simultaneously.

Of the plots gained, it can be observed that the graphs almost match, similar in their behaviors, and in good agreement with each other, especially when considering the integer-order derivative. Indeed, the ABC fractional orders have strong effects on the model profiles, which tend to lead to unusual behaviors in the event of a significant departure from the integer value of $\beta = 1$.

Finally, as the saying goes, it ended with a refreshing scent; the attitude evaluation of $|u(t_i) - u^{21}(t_i)|$ and $|u(t_i) - u^{21}(t_i)||u(t_i)|^{-1}$ are examined. Aught, at various $t_i \in A$ and when $\beta = 1$; Fig. 2 gives the relevant ploted data of the RKA elements in terms of absolute errors; whilst, Fig. 3 describes the relative errors both for Applications 1, 2, and 3, simultaneously. It is seen that the expansion in the quantity of hub brings about a decrease in the total errors and correspondingly an improvement in the exactness of the obtained solutions.

6. HIGHLIGHT AND CONCLUSION

In this research, the damping VDP model are presented and discussed in the emotion of ABC fractional tactic. In this tactic, the RKA is presented and fitted to attain a numerical approximation to three ABC fractional damping VDP models coming from the real-world applications so as to validate and verify our new approach. Meanwhile, two computational algorithms concerned to characterize the given ABC tactic and RKA solutions. Finally, those proposed novel extended and numerical results acquired show the full precision and performance of such adaptation, which can be utilized effectively as an alternative scheme in solving various types of problems under consideration arising in applied mathematics and engineering matters.

ACKNOWLEDGMENT

This research work is supported by the Ajman University grant: 2019–20.

REFERENCES

1. R. Herrmann, *Fractional Calculus*: *An Introduction for Physicists* (World Scientific, Singapore, 2014).
2. V. E. Tarasov, *Fractional Dynamics*: *Applications of Fractional Calculus to Dynamics of Particles*, *Fields and Media* (Springer, Germany, 2011).
3. B. J. West, *Fractional Calculus View of Complexity*: *Tomorrow's Science* (Taylor & Francis, UK, 2015).
4. A. Kilbas, H. Srivastava and J. Trujillo, *Theory and Applications of Fractional Differential Equations* (Elsevier, Netherlands, 2006).
5. B. J. West, *Natures Patterns and the Fractional Calculus* (De Gruyter, Germany, 2017).
6. O. Abu Arqub, Fitted reproducing kernel Hilbert space method for the solutions of some certain classes of time-fractional partial differential equations subject to initial and Neumann boundary conditions, *Comput. Math. Appl.* **73** (2017) 1243–1261.
7. O. Abu Arqub, Numerical solutions for the Robin time-fractional partial differential equations of heat and fluid flows based on the reproducing kernel algorithm, *Int. J. Numer. Methods Heat Fluid Flow* **28** (2018) 828–856.
8. O. Abu Arqub, Solutions of time-fractional Tricomi and Keldysh equations of Dirichlet functions types in Hilbert space, *Numer. Methods Partial Differ. Eq.* **34** (2018) 1759–1780.
9. S. S. Ray, New exact solutions of nonlinear fractional acoustic wave equations in ultrasound, *Comput. Math. Appl.* **71** (2016) 859–868.
10. S. S. Ray and S. Sahoo, Analytical approximate solutions of Riesz fractional diffusion equation and Riesz fractional advection-dispersion equation involving nonlocal space fractional derivatives, *Math. Methods Appl. Sci.* **38** (2015) 2840–2849.
11. M. M. Meerschaert and C. Tadjeran, Finite difference approximations for fractional advection-dispersion flow equations, *J. Comput. Appl. Math.* **172** (2004) 65–77.
12. P. Zhuang, F. Liu, V. Anh and I. Turner, Numerical methods for the variable-order fractional advection-diffusion equation with a nonlinear source term, *SIAM J. Numer. Anal.* **47** (2009) 1760–1781.
13. E. Atilgan, M. Senol, A. Kurt and O. Tasbozan, New wave solutions of time-fractional coupled Boussinesq–Whitham–Broer–Kaup equation as a model of water waves, *China Ocean Eng.* **33** (2019) 477–483.
14. A. Atangana and D. Baleanu, New fractional derivatives with non-local and non-singular kernel: Theory and application to heat transfer model, *Thermal Sci.* **20** (2016) 763–769.
15. A. Atangana and J. J. Nieto, Numerical solution for the model of RLC circuit via the fractional derivative without singular kernel, *Adv. Mech. Eng.* **7** (2015) 1–7.
16. A. Atangana and D. Baleanu, New fractional derivatives with non-local and non-singular kernel: Theory

and application to heat transfer model, *Thermal Sci.* **20** (2016) 763–769.
17. A. Atangana and J. F. Gómez-Aguilar, Decolonisation of fractional calculus rules: Breaking commutativity and associativity to capture more natural phenomena, *Eur. Phys. J. Plus* **133** (2018) 1–22.
18. O. Abu Arqub, Numerical solutions of systems of first-order, two-point BVPs based on the reproducing kernel algorithm, *Calcolo* **55** (2018) 1–28.
19. O. Abu Arqub and B. Maayah, Modulation of reproducing kernel Hilbert space method for numerical solutions of Riccati and Bernoulli equations in the Atangana–Baleanu fractional sense, *Chaos Solitons Fractals* **125** (2019) 163–170.
20. O. Abu Arqub and B. Maayah, Numerical solutions of integrodifferential equations of Fredholm operator type in the sense of the Atangana–Baleanu fractional operator, *Chaos Solitons Fractals* **117** (2018) 117–124.
21. O. Abu Arqub and B. Maayah, Fitted fractional reproducing kernel algorithm for the numerical solutions of ABC-fractional Volterra integro-differential equations, *Chaos Solitons Fractals* **126** (2019) 394–402.
22. J. D. Djida, A. Atangana and I. Area, Numerical computation of a fractional derivative with non-local and non-singular kernel, *Math. Modelling Nat. Phenomena* **12** (2017) 4–13.
23. A. Atangana and J. F. Gómez-Aguilar, Fractional derivatives with no-index law property: Application to chaos and statistics, *Chaos Solitons Fractals* **114** (2018) 516–535.
24. A. Atangana, On the new fractional derivative and application to nonlinear Fisher's reaction-diffusion equation, *Appl. Math. Comput.* **273** (2016) 948–956.
25. A. Atangana and I. Koca, On the new fractional derivative and application to Nonlinear Baggs and Freedman model, *J. Nonlinear Sci. Appl.* **9** (2016) 2467–2480.
26. O. Algahtani, Comparing the Atangana–Baleanu and Caputo–Fabrizio derivative with fractional order: Allen Cahn model, *Chaos Solitons Fractals* **89** (2016) 552–559.
27. B. Vander Pol, A theory of the amplitude of free and forced triode vibrations, *Radio Rev.* **1** (1920) 701–710.
28. H. Jafari, C. M. Khalique and M. Nazari, An algorithm for the numerical solution of nonlinear fractional-order Van der Pol oscillator equation, *Math. Comput. Modelling* **55** (2012) 1782–1786.
29. Z. Guo, A. Y. T. Leung and H. X. Yang, Oscillatory region and asymptotic solution of fractional van der Pol oscillator via residue harmonic balance technique, *Appl. Math. Modelling* **35** (2011) 3918–3925.
30. Y. Xu and O. P. Agrawal, Models and numerical schemes for generalized van der Pol equations, *Commun. Nonlinear Sci. Numer. Simul.* **18** (2013) 3575–3589.
31. M. Kavyanpoor and S. Shokrollahi, Challenge on solutions of fractional Van Der Pol oscillator by using the differential transform method, *Chaos Solitons Fractals* **98** (2017) 44–45.
32. S. Cai and M. Xiao, Boundary observability of wave equations with nonlinear van der Pol type boundary conditions, *Automatica* **98** (2018) 350–353.
33. S. S. Ray and A. Patra, Haar wavelet operational methods for the numerical solutions of fractional order nonlinear oscillatory Van der Pol system, *Appl. Math. Comput.* **220** (2013) 659–667.
34. M. Cui and Y. Lin, *Nonlinear Numerical Analysis in the Reproducing Kernel Space* (Nova Science, USA, 2009).
35. A. Berlinet and C. T. Agnan, *Reproducing Kernel Hilbert Space in Probability and Statistics* (Kluwer Academic Publishers, USA, 2004).
36. A. Daniel, *Reproducing Kernel Spaces and Applications* (Springer, Basel, 2003).
37. O. Abu Arqub, Numerical algorithm for the solutions of fractional order systems of Dirichlet function types with comparative analysis, *Fund. Inf.* **166** (2019) 111–137.
38. W. Jiang and Z. Chen, A collocation method based on reproducing kernel for a modified anomalous subdiffusion equation, *Numer. Methods Partial Differ. Eq.* **30** (2014) 289–300.
39. F. Z. Geng, S. P. Qian and S. Li, A numerical method for singularly perturbed turning point problems with an interior layer, *J. Comput. Appl. Math.* **255** (2014) 97–105.
40. Y. Lin, M. Cui and L. Yang, Representation of the exact solution for a kind of nonlinear partial differential equations, *Appl. Math. Lett.* **19** (2006) 808–813.
41. Y. Zhoua, M. Cui and Y. Lin, Numerical algorithm for parabolic problems with non-classical conditions, *J. Comput. Appl. Math.* **230** (2009) 770–780.
42. A. Akgül, A novel method for a fractional derivative with non-local and non-singular kernel, *Chaos Solitons Fractals* **114** (2018) 478–482.

Fractals 2020.28. Downloaded from www.worldscientific.com by 157.51.20.200 on 08/09/21. Re-use and distribution is strictly not permitted, except for Open Access articles.